

On the coefficients of the liquid drop model mass formulae and nuclear radii

G. Royer¹

*Laboratoire Subatech, UMR: IN2P3/CNRS-Université-Ecole des Mines,
4 rue A. Kastler, 44307 Nantes Cedex 03, France*

Abstract

The coefficients of different mass formulae derived from the liquid drop model and including or not the curvature energy, the diffuseness correction to the Coulomb energy, the charge exchange correction term, different forms of the Wigner term and different powers of the relative neutron excess $I = (N - Z)/A$ have been determined by a least square fitting procedure to 2027 experimental atomic masses. The Coulomb diffuseness correction Z^2/A term or the charge exchange correction $Z^{4/3}/A^{1/3}$ term plays the main role to improve the accuracy of the mass formula. The Wigner term and the curvature energy can also be used separately for the same purpose. The introduction of an $|I|$ dependence in the surface and volume energies improves slightly the efficiency of the expansion and is more effective than an I^4 dependence. Different expressions reproducing the experimental nuclear charge radius are provided. The different fits lead to a surface energy coefficient of around 17-18 MeV and a relative equivalent rms charge radius r_0 of 1.22-1.23 fm.

PACS: 21.10.Dr; 21.60.Ev; 21.60.Cs

Keywords: Mass formula, liquid drop model, Wigner term, charge radius, curvature energy.

¹ E-mail:royer@subatech.in2p3.fr

1 Introduction

The binding energy of new nuclides both in the superheavy element region and the regions close to the proton and neutron drip lines are still poorly known and the different theoretical extrapolations do not fully agree. Therefore other studies are still necessary to better predict the masses of such exotic nuclei. The atomic nucleus resembling to a charged liquid drop, semi-macroscopic models including a pairing energy term have been firstly advanced to determine the nuclear masses [1,2]. Macroscopic-microscopic approaches, mainly the finite-range droplet model and the finite-range liquid drop model [3] have been proposed to simulate the smooth part of the nuclear masses and the non smooth part depending on the parity of the proton and neutron numbers and the proximity of the magic numbers. Nuclear masses have also been reproduced accurately within the statistical Thomas-Fermi model within a Seyler-Blanchard effective interaction [4,5]. Microscopic Hartree-Fock self-consistent calculations using the mean-field approach and Gogny or Skyrme forces and pairing correlations [6,7] as well as relativistic mean field theories [8] have also been advanced to try to reproduce these nuclear masses. Neural networks have been recently used [9] in the same purpose.

Beyond the description of the nuclear ground state energy, the evolution of the nuclear binding energy with deformation and rotation governs the fission, fusion, cluster and α decay potential barriers and the existence of the well deformed rotating states. Within the liquid drop model approach, the main characteristics of these barriers may be reproduced using, firstly, four basic macroscopic terms : the volume, surface, Coulomb and nuclear proximity energy terms and, secondly, shell and pairing energy contributions to explain structure effects and improve quantitatively the results [10,11,12,13,14,15].

In a first paper [16] some coefficients and terms of the liquid drop model mass formula and a specific nuclear radius have been fitted using a set of 1522 experimental nuclear masses. The purpose of the present work is to extend this investigation to determine the relative efficiency of different more complex combinations of terms of the liquid drop model to reproduce the masses [17] of 2027 nuclei and to study, particularly, the separated influence of the curvature energy, the different forms of the Wigner term and of different powers of the relative neutron excess $I = (N - Z)/A$. As suggested in [18] fits on ground state masses alone have been preferred as was done with the Hartree-Fock mass formulae to avoid that the parameters might be distorted by the theoretical and experimental uncertainties associated with the barriers. The second aim is to fit the experimental nuclear charge radii by different expressions and to compare with the relative charge radii $r_0 = R_0/A^{1/3}$ derived from the different mass formulae. Finally, the coefficients of the mass formulae using these different expressions for the charge radius are determined as

well as their accuracy. Another motivation of this work is to improve later the coefficients of the generalized liquid drop model previously proposed [11]. Recently, the mutual influence of terms in semi-empirical formulae has been deeply investigated [19].

2 Nuclear binding energy

The nuclear binding energy $B_{nucl}(A,Z)$ is the energy needed for separating all the nucleons constituting a nucleus. It is related to the nuclear mass $M_{n.m}$ by

$$B_{nucl}(A, Z) = Zm_P + Nm_N - M_{n.m}(A, Z). \quad (1)$$

$B_{nucl}(A,Z)$ may thus be connected to the experimental atomic masses given in [17] since :

$$M_{n.m}(A, Z) = M_{a.m}(A, Z) - Zm_e + B_e(Z). \quad (2)$$

The binding energy $B_e(Z)$ of all removed electrons is [18]

$$B_e(Z) = a_{el}Z^{2.39} + b_{el}Z^{5.35}, \quad (3)$$

with $a_{el} = 1.44381 \times 10^{-5}$ MeV and $b_{el} = 1.55468 \times 10^{-12}$ MeV.

Different subsets of the following expansion of the nuclear binding energy in powers of $A^{-1/3}$ and $|I|$ have been considered :

$$\begin{aligned} B = & a_v \left(1 - k_{v_1}|I| - k_{v_2}I^2 - k_{v_3}I^4\right) A - a_s \left(1 - k_{s_1}|I| - k_{s_2}I^2 - k_{s_3}I^4\right) A^{\frac{2}{3}} \\ & - a_k \left(1 - k_{k_1}|I| - k_{k_2}I^2 - k_{k_3}I^4\right) A^{\frac{1}{3}} - a_0A^0 - \frac{3}{5} \frac{e^2 Z^2}{R_0} + f_p \frac{Z^2}{A} + a_{c,exc} \frac{Z^{\frac{4}{3}}}{A^{\frac{1}{3}}} \\ & - E_{pair} - E_{shell} - E_{Wigner}. \end{aligned} \quad (4)$$

The first term gives the volume energy corresponding to the saturated exchange force and infinite nuclear matter. I^2A is the asymmetry energy of the Bethe-Weizsäcker mass formula. The second term is the surface energy. It takes into account the deficit of binding energy of the nucleons at the nuclear surface and corresponds to semi-infinite nuclear matter. The Bethe-Weizsäcker mass formula does not consider the dependence of the surface energy on I . This term was originally contained in the Weizsäcker formula [1]. The third term is the curvature energy. It is a correction to the surface energy resulting from local properties and consequently depending on the mean local curvature. This

term is considered in the Lublin-Strasbourg Drop (LSD) model [20], the TF model [5] but not in the FRLDM [3]. In the three first terms a dependence on $|I|$ and I^4 , the so-called malacodermous term, has been envisaged since they have been proposed to better reproduce the fission barrier heights [21] and to simulate the softening of the surface of highly neutron-rich nuclei [22]. The A^0 term appears when the surface term is extended to include higher order terms in $A^{-1/3}$ and I . The fifth term gives the decrease of binding energy due to the repulsion between the protons. In the Bethe-Weizsäcker mass formula this Coulomb energy is proportional to $Z(Z - 1)$. Different formulae will be assumed for the charge radius. The Z^2/A term is the diffuseness correction to the basic sharp radius Coulomb energy term (called also the proton form-factor correction to the Coulomb energy in [3]) and the term proportional to $Z^{4/3}/A^{1/3}$ is the charge exchange correction term.

The pairing energy has been calculated with the following expressions used for spherical nuclei in the recent version of the Thomas-Fermi model [5]. For odd Z , odd N and $N=Z$ nuclei

$$E_{Pair} = 4.8/N^{1/3} + 4.8/Z^{1/3} - 6.6/A^{2/3} - 30/A \text{ MeV}. \quad (5)$$

For odd Z , odd N and $N \neq Z$ nuclei

$$E_{Pair} = 4.8/N^{1/3} + 4.8/Z^{1/3} - 6.6/A^{2/3} \text{ MeV}. \quad (6)$$

For odd Z , even N nuclei

$$E_{Pair} = 4.8/Z^{1/3} \text{ MeV}. \quad (7)$$

For even Z , odd N nuclei

$$E_{Pair} = 4.8/N^{1/3} \text{ MeV}. \quad (8)$$

For even Z , even N nuclei

$$E_{Pair} = 0. \quad (9)$$

The theoretical shell effects used in the TF model (7th column of the table in [4] and [5]) have also been retained since they allow to reproduce correctly the masses from fermium to $Z = 112$ [23]. They have been calculated from the Strutinsky shell-correction method and previously to the other coefficients of the TF model. The fits on nuclear masses depend necessarily on the choice of the selected theoretical shell effects or the formulae chosen to

describe these shell effects. The sign for the shell energy term comes from the adopted definition in [4]. It gives, for example, a contribution of 12.84 MeV to the binding energy of ^{208}Pb .

The Wigner energy allows to reproduce the kink in the nuclear mass surface that is not a shell effect in the usual sense. It depends on I and appears in the counting of identical pairs in a nucleus. Different expressions are considered. The first expression is simply $W|I|$ [24]. Its effect is to decrease the binding energy when $N \neq Z$.

The congruence energy term is given by :

$$E_{cong} = -10 \exp(-4.2|I|) \text{ MeV}. \quad (10)$$

It represents an extra binding energy associated with the presence of congruent pairs [5].

Within an Hartree-Fock approach [25] it has been assumed that there is nothing compelling about an exponential representation and a gaussian expression

$$E = V_W \exp(-\lambda I^2) \quad (11)$$

is just as acceptable.

Another term has also been proposed in [25]

$$E = \beta |N - Z| \exp \left[-(A/A_0)^2 \right]. \quad (12)$$

We have also tested separately two other possible expressions

$$E = \beta |N - Z| \exp \left[-(A/A_0) \right]. \quad (13)$$

and

$$E = \beta \frac{|N - Z|}{1 + (A/A_0)^2}. \quad (14)$$

The term of nuclear proximity energy does not appear in the binding energy of the ground state since it becomes effective only for necked shapes but not for slightly deformed ground states.

3 Coefficients of the mass formulae

To obtain the coefficients of the different expansions by a least square fitting procedure, the masses of the 2027 nuclei verifying the two conditions : N and Z higher than 7 and the one standard deviation uncertainty on the mass lower than or equal to 150 keV [17] have been used. These restrictions are not employed by all investigators [19,26]. The root-mean-square deviation σ defined by

$$\sigma^2 = \frac{\sum [M_{Th} - M_{Exp}]^2}{n} \quad (15)$$

has been used to determine the relative efficiency of the different selected sets of terms since $n \gg f$ where f is the number of fit parameters. A very efficient software has been used. The extraction of standard errors on the fit parameters seems very difficult but the errors are surely very weak. On the other hand, the values of the last decimals of a coefficient can be changed in counterbalancing by a change in the last decimals of another coefficient for almost the same rms deviation.

In Table I, the improvement of the nuclear mass reproduction when additional contributions are added to the basic A , AI^2 , $A^{2/3}$, $A^{2/3}I^2$, $Z^2/A^{1/3}$ terms is clearly displayed. The curvature energy is not taken into account. The introduction of the pairing term is obviously necessary. The introduction of a constant term improves slightly the adjustment and changes strongly the surface energy coefficient. It induces also a severe discontinuity during the transition from one to two-body shapes as in fission, fusion or α emission. The congruence energy term at least with the fixed coefficients adopted here (as in the LSD and TF models) is much less efficient to lower σ than the Wigner term $W|I|$. When the coefficients before the exponential and the exponent are free the congruence energy tends to the usual Wigner term since the coefficient before the exponential diminishes while the exponent increases. The diffuseness correction to the Coulomb energy and the standard Wigner term $W|I|$ can be used separately to strongly lower σ . The Wigner energy is approximately independent of the nuclear shape [24]. In a division into 2 fragments, all with the same value of $|I|$, the form $W|I|$ for the Wigner energy jumps at scission to 2 times its original value, which leads to a discontinuity of around 6.7 MeV of the potential energy at the scission point between the nascent fragments for ^{258}Fm as an example. For the congruence energy the discontinuity is also important : 3.9 MeV for this same nucleus. The Coulomb diffuseness correction term has the main advantage to be almost continuous at the scission point in the entrance or exit channels. The combination of the Coulomb diffuseness correction term and the $W|I|$ term allows to reach the very satisfactory value $\sigma = 0.608$ [3,7,20]. The $A^{2/3}|I|$ term is useful to improve

the accuracy of the expansion and is more effective than the $A^{2/3}I^4$ term but when the Wigner term and the Coulomb diffuseness correction factor term are taken into account the introduction of the $A^{2/3}|I|$, $A^{2/3}I^4$ and A^0 terms are ineffective.

In Table II, the efficiency of the curvature energy term with different I dependences is investigated without taking into account the Wigner contribution. When the Coulomb diffuseness correction is disregarded the introduction of the term in $A^{1/3}$ allows to decrease σ of 0.1 MeV. When the Coulomb diffuseness correction is considered the term in $A^{1/3}$ is ineffective. The addition of a $A^{1/3}I^2$ term improves slightly the results. Supplementary terms in $|I|$ to calculate the volume, surface and curvature energies allow finally to reach $\sigma=0.58$ MeV. They are still more efficient than the I^4 terms. The curvature energy has the advantage to be continuous at the scission point at least in symmetric entrance or decay channels. It has the disadvantage that its value (and its sign) lacks of stability.

These two first tables show a good convergency of the volume a_v and asymmetry volume k_v constants respectively towards around 15.5 MeV and 1.7–1.9. The variation of the surface coefficient is larger but a_s evolves around 17-18 MeV. Small values of the surface coefficient favors quasi-molecular or two-body shapes at the saddle-point of the potential barriers while large values of a_s promote one-body elongated shapes. As it is well known the surface asymmetry coefficient k_s is less easy to precise.

For the Bethe-Weizsäcker formula the fitting procedure leads to

$$B_{nucl}(A, Z) = 15.5704A - 17.1215A^{2/3} - 0.71056 \frac{Z(Z-1)}{A^{1/3}} - 23.4496I^2A - E_{pair} - E_{shell} \quad (16)$$

with $\sigma=1.30$ MeV. That gives $r_0=1.216$ fm and $k_v=1.506$. The σ value is explained by the non dependence of the surface energy term on the relative neutron excess I .

The mass formulae including a Wigner term given by the formulae (12),(13) or (14) are examined in Table III. The values of A_0 which minimize the mass rms deviation are respectively 48, 35 and 40 for these three expressions. They are determined with an accuracy of around 5 mass numbers. These formulas for the Wigner energy are supposed to be approximately independent of the nuclear shape. Their discontinuity at the scission point of fission or fusion barriers is less important than that of the congruence and $W|I|$ terms. For example, for the expressions $|N-Z| \exp[-(A/48)^2]$, $1.5|N-Z| \exp[-(A/35)]$ and $1.6 \frac{|N-Z|}{1+(A/40)^2}$ and symmetric decay of the ^{254}Fm the discontinuities at the contact point of the nascent fragments are respectively 0, 0.05 and 2.2 MeV.

The first, fifth and eighth lines of the table indicate that within the simplest form for the volume and surface energies, thus with only 7 parameters, the r.m.s deviation on the masses is less than 0.6 MeV. The introduction of a dependence on $|I|$ and of the curvature energy lowers σ of 0.04 MeV within the expression (12) and of 0.02 MeV for the two last ones. The surface energy coefficients are generally lower with these forms of the Wigner energy and, consequently, r_0 is generally higher.

Within the Wigner term derived from the Hartree-Fock approach [6] and taking $A_0 = 28$ and $\lambda = 485$ in the formulas (11) and (12) as derived using the BSk2 Skyrme force the following formula is obtained

$$\begin{aligned}
B = & 15.4503 \left(1 - 1.7463I^2\right) A - 17.5701 \left(1 - 1.5296I^2\right) A^{2/3} \\
& - \frac{0.6e^2 Z^2}{1.219A^{1/3}} + 1.1948 \frac{Z^2}{A} - E_{pair} - E_{shell} + 1.769e^{-485I^2} \\
& - 0.2197|N - Z|e^{-(A/28)^2}
\end{aligned} \tag{17}$$

with $\sigma = 0.623 \text{ MeV}$.

The accuracy can be improved in varying A_0 and λ :

$$\begin{aligned}
B = & 15.4121 \left(1 - 1.7972I^2\right) A - 17.3059 \left(1 - 1.7911I^2\right) A^{2/3} \\
& - \frac{0.6e^2 Z^2}{1.232A^{1/3}} + 0.8961 \frac{Z^2}{A} - E_{pair} - E_{shell} + 2.25e^{-80I^2} \\
& - 0.4883|N - Z|e^{-(A/50)^2}
\end{aligned} \tag{18}$$

It leads to $\sigma = 0.573 \text{ MeV}$ and produces sizable changes in several of the other parameters which proves the importance of the Wigner term and the mutual influence of terms in the semi-empirical mass formulae [19].

In Table IV the efficiency of the charge exchange correction term in $Z^{4/3}/A^{1/3}$ is studied. The lines can be compared respectively to the 7th line of table 1, 2nd line of table 2, 8th line of table 1, 3rd line of table 2, 6th and 12th lines of table 1 and 1st and 5th lines of table 3. The only change is that the diffuseness correction term in Z^2/A has been replaced by the charge exchange correction term. It is quite interesting to observe that the introduction of these two terms separately leads to the same accuracy, the same value of the charge radius, almost the same values of the surface coefficients and to small changes of the volume coefficients. So the charge exchange correction term is as efficient as the diffuseness correction term and there is no correlation between these two terms and the charge radius and the surface coefficients and weak correlation with the volume coefficients. The introduction of both these two terms does not allow to improve the accuracy of the mass formulae

and leads to spurious values of the volume coefficient.

Finally, the shell and pairing energies, the diffuseness correction term to the Coulomb energy, the charge exchange correction term and the Wigner energy separately lead to significant reductions of the rms deviation while the other terms increase the accuracy by only 2 or 3 per cent. A correlation between the surface coefficient and the radius can be extracted. The relative radius r_0 diminishes when the surface coefficient increases.

4 Nuclear charge radius

Experimentally and for nuclei verifying N and Z higher than 7 the set of 782 ground state nuclear charge radii presented in ref. [27] indicates a rms charge radii of $0.94944A^{1/3}$ which leads for the equivalent rms charge radius (denoted by Q in ref. [28]) given by

$$R_0 = \sqrt{\frac{5}{3}} \langle r^2 \rangle^{1/2} \quad (19)$$

to the value $R_0 = 1.2257 A^{1/3} fm$ with $\sigma = 0.124 fm$. Other data have been obtained recently [29]. In the adjustment to the nuclear masses displayed in the tables I and II the reduced charge radius $r_{0,charge}$ converges to 1.22-1.23 fm in good agreement with the experimental data for the charge radius. The introduction of the expressions (12), (13) and (14) for the Wigner term leads to slightly higher values.

The experimental data indicate that the ratio $R_0/A^{1/3}$ is not strictly constant. For example, $R_0/A^{1/3} = 1.312 fm$ for ^{40}Ca and $R_0/A^{1/3} = 1.234$ for ^{48}Ca while $R_0/A^{1/3} = 1.217$ for ^{190}Pb and $R_0/A^{1/3} = 1.201 fm$ for ^{214}Pb . These R_0 and r_0 values correspond to the Coulomb energy of a charged liquid drop with constant charge density and spherical sharp surface. It must not be confused with half-density radius derived from two-parameter Fermi function or other parameters entering in other parametrisations of the charge distribution.

In the adjustment to the experimental nuclear masses the nuclear mass radius is not fitted. Root-mean-squared matter radii are given in Ref. [30] for specific nuclei. For all isotopic series a decrease of the mass rms radius is observed with increasing neutron number as for the charge radius. In this mass range ($A = 63 - 75$) the radius of the neutron and proton distributions are very similar. Global fits lead to an overall contraction of the nuclear radius as $T = |N - Z|/2$ increases [31], a so called "isospin shrinkage". Recently, an

estimate of the neutron skin linear in the relative neutron excess I has been extracted from experimental proton radii and observed mirror displacement energies [32] and the coefficients have been also determined from antiprotonic X-rays and radiochemical data [33].

Within a simple form of the mass formula including the Coulomb diffuseness correction and the Wigner term given by the formula (13) but not the dependence on the curvature energy and on $|I|$ and I^4 the introduction of the factor $r_0 = 1.2257$ deduced from the experimental charge radius leads to

$$B = 15.3543 (1 - 1.7445I^2) A - 17.2293 (1 - 1.5765I^2) A^{2/3} - \frac{0.6e^2Z^2}{1.2257A^{1/3}} + 1.2442 \frac{Z^2}{A} - E_{pair} - E_{shell} - 0.7641|N - Z|e^{-A/35} \quad (20)$$

and $\sigma = 0.615 \text{ MeV}$.

More accurate formulae may be used to reproduce the mean behaviour of the equivalent rms charge radius.

The expression

$$R_0 = 1.0996A^{1/3} + 0.653 \text{ fm} \quad (21)$$

leads to $\sigma = 0.066 \text{ fm}$. Its introduction in the above-mentioned mass formula curiously diminishes the accuracy to $\sigma = 1.16 \text{ MeV}$. The same behaviour is observed when the dependence in Z^2/A is replaced by a dependence in $Z^{4/3}/A^{1/3}$.

The formula

$$R_0 = 1.1718A^{1/3} + \frac{1.4069}{A^{1/3}} \text{ fm} \quad (22)$$

leads to $\sigma = 0.064 \text{ fm}$, while for the corresponding mass formula $\sigma = 0.929 \text{ MeV}$.

The adjustment to the experimental charge radii within the form proposed in Ref.[34] gives

$$R_0 = 1.1818A^{1/3} - 0.089 + \frac{1.5938}{A^{1/3}} \text{ fm} \quad (23)$$

with $\sigma = 0.064 \text{ fm}$ and $\sigma = 0.900 \text{ MeV}$ while the form selected in Ref.[35] leads to

$$R_0 = 1.1769A^{1/3} + \frac{1.2046}{A^{1/3}} + \frac{1.5908}{A} fm \quad (24)$$

and $\sigma = 0.064 fm$ for the radius and $0.88 MeV$ for the corresponding mass formula.

The form of the expression given the equivalent rms charge radius proposed in Ref.[36]

$$R_0 = 1.2332A^{1/3} + \frac{2.8961}{A^{2/3}} - 0.18688A^{1/3}I fm \quad (25)$$

gives a good accuracy $\sigma = 0.052 fm$ but $\sigma = 0.765 MeV$.

The fact that improved formulae for the charge radius lead to significantly poorer fits to the masses calls into question the reliability of the equivalent uniform charge distribution as a link between charge radii and Coulomb energy.

Finally a rms deviation for the charge radius of only 0.01 fm (fitted on 362 nuclei) has been obtained in Ref. [31] in expressing the charge mean square radius by

$$r^3 = a + bA + cT \quad (26)$$

for spherical nuclei and taking into account the deformation for the other nuclei via a nucleonic promiscuity form factor P depending on the distance of Z and N to the proton and neutron magic numbers.

To describe the main properties of the fusion, fission, cluster and α emission potential barriers in the quasi-molecular shape path, the formula

$$R_0 = 1.28A^{1/3} - 0.76 + 0.8A^{-1/3} \quad (27)$$

proposed in Ref.[34] for the equivalent rms radius has been retained in the GLDM [10,11,12,13,14,15,16]. This formula coming from the Droplet Model approach simulated a small decrease of the density with increasing mass. This does not seem corroborated by the experimental data [27] at least on the charge radius. Nevertheless without changing the surface and Coulomb energies which are shape-dependent terms, the adjustment of the volume energy coefficients and the introduction of a pure Wigner term leads to

$$B = 15.5209 \left(1 - 1.934I^2\right) A - 17.9439 \left(1 - 2.6I^2\right) A^{2/3} - \frac{0.6e^2 Z^2}{1.28A^{1/3} - 0.76 + 0.8A^{-1/3}} + 2.1798 \frac{Z^2}{A} - E_{pair} - E_{shell} - 27.21|I| \quad (28)$$

and $\sigma = 0.686 \text{ MeV}$. The introduction of other terms can still allow to diminish σ .

The Fig. 1 displays the difference between the theoretical and experimental masses within a formula of Table I recalled below :

$$\begin{aligned}
 B &= 15.3543 \left(1 + 0.0284|I| - 1.8837I^2 \right) A \\
 &\quad - 17.0068 \left(1 + 0.131|I| - 2.274I^2 \right) A^{2/3} \\
 &\quad - \frac{0.6e^2 Z^2}{1.228A^{1/3}} + 1.0339 \frac{Z^2}{A} - E_{pair} - E_{shell} - 16.27|I|
 \end{aligned} \tag{29}$$

with $\sigma = 0.605 \text{ MeV}$. For most of the nuclei with A higher than 110 the difference between the theoretical and experimental masses is less than 1 MeV.

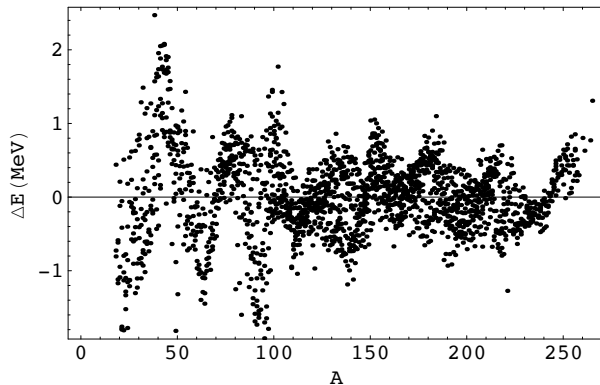


Fig. 1. Difference (in MeV) between the theoretical and experimental masses for the 2027 selected nuclei as a function of the mass number.

5 Summary and conclusion

The coefficients of different mass formulae derived from the liquid drop model and including or not the curvature energy, the Coulomb diffuseness correction energy, the charge exchange correction term, different forms of the Wigner term and different powers of the relative neutron excess I have been determined by a least square fitting procedure to 2027 experimental atomic masses.

The Coulomb diffuseness correction Z^2/A term or the charge exchange correction $Z^{4/3}/A^{1/3}$ term plays the main role to improve the accuracy of the mass formula. The Wigner term and, with a smaller effect, the curvature energy can also be used separately for the same purpose but their coefficients are

unstable. The introduction of an $|I|$ dependence in the surface and volume energies improves only slightly the efficiency of the expansion. An I^4 dependence and a constant term are not worth including. Expressions for the Wigner term leading to small discontinuities at the scission point of the potential barriers are as efficient as the $W|I|$ term. Different expressions reproducing the experimental nuclear charge radius are provided. The different fits lead to a surface energy coefficient of around 17-18 MeV and a relative equivalent rms charge radius r_0 of 1.22-1.23 fm.

References

- [1] C.F. von Weizsäcker, Z. Physik 96 (1935) 431.
- [2] H.A. Bethe, R.F. Bacher, Rev. Mod. Phys. 8 (1936) 82.
- [3] P. Möller, J.R. Nix, W.D. Myers, W.J. Swiatecki, At. Data Nucl. Data Tables 59 (1995) 185.
- [4] W.D. Myers, W.J. Swiatecki, LBL report 36803, 1994.
- [5] W.D. Myers, W.J. Swiatecki, Nucl. Phys. A 601 (1996) 141.
- [6] M. Samyn, S. Goriely, P.-H. Heenen, J.M. Pearson, F. Tondeur, Nucl. Phys. A 700 (2002) 142.
- [7] J. Rikovsky Stone, J. Phys. G 31 (2005) R211.
- [8] M. Bender, et al., Phys. Lett. B 515 (2001) 42.
- [9] S. Athanassopoulos, E. Mavrommatis, K.A. Gernoth, J.W. Clark, Nucl. Phys. A 743 (2004) 222.
- [10] G. Royer, B. Remaud, J. Phys. G 10 (1984) 1057.
- [11] G. Royer, B. Remaud, Nucl. Phys. A 444 (1985) 477.
- [12] G. Royer, J. Phys. G 26 (2000) 1149.
- [13] G. Royer, R. Moustabchir, Nucl. Phys. A 683 (2001) 182.
- [14] R.A. Gherghescu, G. Royer, Phys. Rev. C 68 (2003) 014315.
- [15] C. Bonilla, G. Royer, Heavy Ion Phys. 25 (2006) 11.
- [16] G. Royer, C. Gautier, Phys. Rev. C 73 (2006) 067302.
- [17] G. Audi, A.H. Wapstra, C. Thibault, Nucl. Phys. A 729 (2003) 337.
- [18] D. Lunney, J.M. Pearson, C. Thibault, Rev. Mod. Phys. 75 (2003) 1021.
- [19] M. W. Kirson, Nucl. Phys. A 798 (2008) 29.

- [20] K. Pomorski, J. Dudek, Phys. Rev. C 67 (2003) 044316.
- [21] M. Dahlinger, D. Vermeulen, K.H. Schmidt, Nucl. Phys. A 376 (1982) 94.
- [22] A.K. Dutta, J.P. Arcoragi, J.M. Pearson, R.H. Behrman, M. Farine, Nucl. Phys. A 454 (1986) 374.
- [23] S. Hofmann, et al., Z. Phys. A 354 (1996) 229.
- [24] W.D. Myers, Droplet Model of Atomic Nuclei, Plenum, New York, 1977.
- [25] S. Goriely, M. Samyn, P.-H. Heenen, J.M. Pearson, F. Tondeur, Phys. Rev. C 66 (2002) 024326.
- [26] A.E.L. Dieperink, P. Van Isacker, Eur. Phys. J. A 32 (2007) 11.
- [27] I. Angeli, At. Data Nucl. Data Tables 87 (2004) 185.
- [28] R.W. Hasse, W.D. Myers, Geometrical relationships of macroscopic nuclear physics, Springer-Verlag, Berlin, 1988.
- [29] J. Libert, B. Roussière, J. Sauvage, Nucl. Phys. A 786 (2007) 47.
- [30] G.F. Lima, et al., Nucl. Phys. A 735 (2004) 303.
- [31] J. Duflo, Nucl. Phys. A 576 (1994) 29.
- [32] J. Duflo, A.P. Zucker, Phys. Rev. C 66 (2002) 051304(R).
- [33] E. Friedman, A. Gal, J. Mareš, Nucl. Phys. A 761 (2005) 283.
- [34] J. Blocki, J. Randrup, W.J. Swiatecki, C.F. Tsang, Ann. of Phys. 105 (1977) 427.
- [35] P.A. Seeger, W.M. Howard, Nucl. Phys. A 238 (1975) 491.
- [36] W.D. Myers, W.J. Swiatecki, Phys. Rev. C 62 (2000) 044610.

Table 1

Dependence of the energy coefficient values (in MeV or fm) on the selected term set including or not the pairing and congruence terms and root mean square deviation. The theoretical shell energies are taken into account but not the curvature energy. The Coulomb energy is determined by $a_c \frac{Z^2}{A^{1/3}}$ with $a_c = 3e^2/5r_0$.

a_v	k_{v1}	k_{v2}	k_{v3}	a_s	k_{s1}	k_{s2}	k_{s3}	a_0	W	$Cong$	$Pair$	r_0	f_p	σ
15.5959	-	1.7051	-	17.1723	-	0.994	-	-	-	n	n	1.227	-	1.32
15.4996	-	1.7011	-	16.7628	-	0.990	-	-	-	n	y	1.235	-	0.977
15.0775	-	1.6799	-	14.8548	-	1.005	-	7.686	-	n	y	1.269	-	0.917
15.93	-	1.8454	-	18.7399	-	1.722	-	-	-	y	y	1.204	-	0.870
15.3416	-	1.8220	-	16.0795	-	1.838	-	10.982	-	y	y	1.251	-	0.728
15.8559	-	1.8549	-	19.3863	-	1.999	-	-	-	y	y	1.191	1.1478	0.628
15.4108	-	1.7119	-	17.5361	-	1.404	-	-	-	n	y	1.218	1.3755	0.660
15.4721	-	1.7154	-	17.8591	-	1.411	-	-1.2	-	n	y	1.212	1.4358	0.659
15.4436	-	1.5909	2.147	17.4801	-	0.732	10.96	-	-	n	y	1.215	1.2286	0.640
15.4367	-0.0551	1.9205	-	17.2772	-0.296	2.420	-	-	-	n	y	1.215	1.1095	0.616
15.3306	-	1.8991	-	16.1189	-	2.410	-	-	41.82	n	y	1.254	-	0.729
15.351	-	1.8097	-	16.9773	-	1.972	-	-	21.60	n	y	1.233	0.9621	0.608
15.3543	-0.0284	1.8837	-	17.0068	-0.131	2.274	-	-	16.27	n	y	1.228	1.0339	0.605
15.5494	-	1.8406	-	17.9723	-	2.077	-	-4.130	26.08	n	y	1.216	1.0681	0.590
15.3619	-	1.7539	0.799	17.0142	-	1.682	3.88	-	19.57	n	y	1.230	0.9879	0.606

Table 2

Dependence of the energy coefficient values (in MeV or fm) on the selected term set and root mean square deviation. The theoretical pairing and shell energies are included but not the Wigner energy. The Coulomb energy is determined by $a_c \frac{Z^2}{A^{1/3}}$ with $a_c = 3e^2/5r_0$.

a_v	k_{v1}	k_{v2}	k_{v3}	a_s	k_{s1}	k_{s2}	k_{s3}	a_k	k_{k1}	k_{k2}	k_{k3}	r_0	f_p	σ
14.772	-	1.6753	-	12.3434	-	1.094	-	7.602	-	-	-	1.285	-	0.873
15.4623	-	1.7140	-	17.8861	-	1.402	-	-0.564	-	-	-	1.214	1.4157	0.660
15.444	-	1.8730	-	18.0077	-	2.783	-	-1.269	-	47.98	-	1.221	1.3721	0.639
15.4401	-	2.3713	-7.447	17.9965	-	7.136	-65.24	-1.983	-	134.19	-1530.7	1.230	1.1196	0.594
15.7016	0.1622	1.351	-	19.6025	1.223	-1.445	-	-5.116	11.917	-27.66	-	1.220	1.0166	0.583

Table 3

Dependence of the energy coefficient values (in MeV or fm) on the selected term set and root mean square deviation. The theoretical pairing and shell energies are included. The Wigner energy determined by the expressions (12), (13) or (14) are taken into account. The I^4 term is disregarded.

a_v	k_{v_1}	k_{v_2}	a_s	k_{s_1}	k_{s_2}	a_k	k_{k_1}	k_{k_2}	β (12)	β (13)	β (14)	r_0	f_p	σ
15.2565	-	1.7475	16.8485	-	1.603	-	-	-	0.679	-	-	1.241	1.1161	0.600
15.311	-0.035	1.8745	16.826	-0.197	2.238	-	-	-	0.535	-	-	1.235	0.9642	0.580
15.5431	-	1.6662	18.8035	-	0.721	-3.343	-	-12.95	1.017	-	-	1.220	1.2826	0.580
15.8011	0.0752	1.5133	20.0578	0.466	-0.223	-5.754	4.068	-15.75	0.794	-	-	1.213	0.9836	0.556
15.2374	-	1.7880	16.6394	-	1.803	-	-	-	-	1.514	-	1.245	0.9639	0.590
15.2949	-0.0047	1.8077	16.7004	-0.057	1.958	-	-	-	-	1.319	-	1.241	0.8456	0.585
15.3474	0.1082	1.3103	17.3787	0.800	-2.111	-1.789	16.015	-85.97	-	2.249	-	1.247	0.7978	0.571
15.2738	-	1.8238	16.6658	-	2.010	-	-	-	-	-	1.262	1.242	0.8822	0.581
15.315	-	1.7455	16.7943	-	1.150	-0.217	-	-190.59	-	-	1.581	1.238	0.8382	0.574
15.265	0.1212	1.2866	16.8666	0.873	-2.401	-1.041	22.288	-154.51	-	-	2.516	1.254	0.7380	0.563

Table 4

Dependence of the energy coefficient values (in MeV or fm) on the selected term set and root mean square deviation. The theoretical pairing and shell energies are included as well as the charge exchange correction term. The Coulomb energy is determined by $a_c \frac{Z^2}{A^{1/3}}$ with $a_c = 3e^2/5r_0$.

a_v	k_{v2}	a_s	k_{s2}	a_k	k_{k2}	a_0	W	Cong	β (12)	β (13)	r_0	$a_{c,exc}$	σ
15.2393	1.7168	17.5359	1.404	-	-	-	-	-	-	-	1.218	1.2987	0.660
15.2876	1.7191	17.8984	1.402	-0.584	-	-	-	-	-	-	1.214	1.3361	0.660
15.2949	1.7206	17.8647	1.411	-	-	-1.222	-	-	-	-	1.212	1.3530	0.659
15.2752	1.8799	18.0208	2.785	-1.291	47.24	-	-	-	-	-	1.221	1.2934	0.638
15.7124	1.8602	19.3863	1.999-	-	-	-	-	y	-	-	1.191	1.0850	0.628
15.2305	1.8138	16.9776	1.972	-	-	-	21.58	-	-	-	1.233	0.9100	0.608
15.1186	1.7518	16.8486	1.603	-	-	-	-	-	0.678	-	1.241	1.0501	0.600
15.1174	1.7910	16.6395	1.803	-	-	-	-	-	-	1.514	1.245	0.9082	0.589